Cellulose Structural Change in Various Biomass Species Pretreated by Ionic Liquid at Different Biomass Loadings

Takatsugu Endo,[a] Shunsuke Fujii,[b] Ei Mon Aung,[b, c] Kosuke Kuroda,[b] Takayuki Tsukegi,[d] Kazuaki Ninomiya,[e] and Kenji Takahashi [b,*]

High biomass loading is a key technique to reduce the pretreatment cost of lignocellulosic biomass. In this work, various biomass species such as bagasse, erianthus, cedar, and eucalyptus were pretreated using an ionic liquid, 1-ethyl-3-methylimidazolium acetate, at different biomass loadings, particularly focusing on a high loading region. Cellulose structural changes in pretreated biomass were investigated *via* X-ray scattering and ^{13}C solid-state nuclear magnetic resonance (SSNMR) spectroscopy. The structural behaviors roughly fell into two categories, corresponding to either grassy (bagasse and erianthus) or woody (cedar and hardwood) biomass. The grassy biomass gradually transformed from cellulose-I to cellulose-II in a monotonic manner against the biomass loading. In contrast, the transformation in the woody biomass occurred abruptly as solids was decreased within the high loadings range (50 wt% to 33 wt%). Below 33 wt%, a reformation of cellulose-I from cellulose-II proceeded readily. In terms of cellulose crystallinity, erianthus as well as bagasse showed a minimum value at 25 wt% loading, whereas the crystallinity for the woody biomass did not possess such a clear minimum. Acid hydrolysis of these pretreated biomass was also conducted and the relationship between the reactivity and the cellulose structural changes was discussed.

Keywords: Ionic liquid; Pretreatment; High loading; Bagasse; Erianthus; Cedar; Eucalyptus; X-ray; NMR; Acid hydrolysis

*Contact information: a: Department of Molecular Chemistry and Biochemistry, Faculty of Science and Engineering, Doshisha University, 1-3 Tatara Miyakodani, Kyotanabe-Shi, Kyoto-fu 610-0394, Japan; b: Faculty of Natural System, Institute of Science and Engineering, Kanazawa University, Kakuma-Machi, Kanazawa 920-1192, Japan; c: Department of Chemical Engineering, Mandalay Technological University, Patheingyi Township, Mandalay, Myanmar; d: Innovative Composite Materials Research and Development Center (ICC), Kanazawa Institute of Technology, 2-2 Yatsukaho, Haku-San 924-0838, Japan; e: Institute for Frontier Science Initiatives, Kanazawa University, Kakuma-Machi, Kanazawa 920-1192, Japan; *Corresponding author: ktkenji@staff.kanazawa-u.ac.jp*

INTRODUCTION

Ionic liquid (IL) pretreatment is a newly emerged and efficient technique to deconstruct the recalcitrance of lignocellulosic biomass (Wang *et al.* 2012; Brandt *et al.* 2013). The ILs are salts that exist in liquid state at room temperature. Some specifically designed ILs are feasible to dissolve cellulose (Swatloski *et al.* 2002) and even lignocellulose (Kilpeläinen *et al.* 2007). After removing IL from the lignocellulose solution, the regenerated lignocellulose becomes much less recalcitrant. Ionic liquid pretreatments have attracted much attention because of their high efficiency as well as their negligible vapor pressure and flammability. However, the high costs of IL compared to

conventional organic solvents is one of the main impediments for their use (Reddy 2015; Baral and Shah 2016).

A high biomass loading during IL pretreatment is a direct and feasible solution. Normally, *ca.* 5 wt% of biomass loading is employed (Brandt *et al.* 2013), which makes the lignocellulose/IL mixture a viscous solution. Much effort has been devoted to establish higher lignocellulose loadings (Wu *et al.* 2011; Cruz *et al.* 2013; da Silva *et al.* 2013; Haykir and Bakir 2013; Li *et al.* 2013; Ninomiya *et al.* 2013; Qiu *et al.* 2014; Uju *et al.* 2013; Zhang *et al.* 2014; Wang *et al.* 2015; Ren *et al.* 2016) compared to the normal loading amount. In these reports, biomass loading amounts higher than 5 wt% were successfully and consistently used, *e.g.* 30 wt%, which did not decrease the subsequent hydrolysis efficiency. Compared to 5 wt%, a concentration of 30 wt% means that loading times more than eight times higher is feasible when the same amount of IL is used, providing a robust cost reduction. Among these reports, only two studies intriguingly stated that when grassy biomass was used with a certain IL pretreatment condition, it lowered the crystallinity of regenerated cellulose at a higher biomass loading to some extent (Cruz *et al.* 2013; Zhang *et al.* 2014). Because the crystallinity of cellulose is considered a major contributor to the recalcitrance effect, the hydrolysis reactivity could be enhanced at higher loading; however, such a phenomenon was not observed.

Recently, the authors addressed this inconsistency using microcrystalline cellulose as a model compound (Endo *et al.* 2017). It was observed that compared to *ca.* 5 wt% loading, the crystallinity of cellulose declined when 25 wt% to 40 wt% loading was used. A subsequent hydrolysis catalyzed by an enzyme, the common hydrolysis method employed by many other research groups, was not enhanced at the high loadings. In contrast, another hydrolysis route, *viz.* acid hydrolysis, proceeded 1.6 times more efficiently in accordance with the crystallinity change. The structural and morphological investigations revealed that the difference between these catalysts could be attributed to their size. At higher loadings, the pores that formed in the regenerated cellulose were smaller, and hence the access of the enzyme with large molecular size into inner cellulose was restricted. The concept that higher cellulose loading in an IL pretreatment causes lower crystallinity of cellulose and that this consequently enhances the acid hydrolysis efficiency was successfully applied to bagasse (up to 33 wt%) as lignocellulosic biomass (Aung *et al.* 2018), where the cellulose is encapsulated by the other biopolymers.

To expand this concept to other types of biomass, especially woody biomass, in this work the authors focused on the investigations of cellulose structural changes in pretreated biomass in different biomass species. Bagasse is an agricultural residue and a grassy biomass. The three lignocellulosic materials examined in this study were erianthus (grass, but not an agricultural residue), cedar (softwood), and eucalyptus (hardwood). The cellulosic structural changes in biomass, including cellulose crystallinity, a major factor that governs cellulose recalcitrance, were investigated in detail *via* wide angle X-ray scattering (WAXS) and ^{13}C solid-state nuclear magnetic resonance (SSNMR) spectroscopy against various biomass loadings ranging from 5 wt% to 50 wt%. Acid hydrolysis was also performed and the relationship between glucose yield and cellulose structural changes was discussed. It should be noted that the data for bagasse were taken from the authors' previous paper (Aung *et al.* 2018), whereas the WAXS peak analyses and the experiments at 25 wt% loading of bagasse were from the current study.

EXPERIMENTAL

Materials

IL-pretreatment

An IL, 1-ethyl-3-methylimidazolium acetate ([Emim][OAc]) that is the most representative IL for lignocellulose pretreatments, was purchased from IoLiTec (> 95% purity;-Ionic Liquid Technologies GmbH, Heilbronn, Germany). The IL was vacuum-dried overnight at 50 °C before use. The biomass materials, bagasse, cedar, and eucalyptus were purchased from the Toyota Motor Corporation (Miyoshi, Japan), while the National Agriculture and Food Research Organization (Ibaraki, Japan) kindly supplied the erianthus sample. Each lignocellulosic sample was first ground by a mill and then sieved to obtain a powder with a particle diameter of 75 μm to 125 μm. The powdered sample was vacuum-dried at 70 °C for 3 h to eliminate adsorbed moisture. The chemical composition of the lignocellulosic sample was then analyzed according to the National Renewable Energy Laboratory (NREL) method (Sluiter *et al.* 2012) as described in the previous paper (Aung *et al.* 2018). The measurements were recorded in triplicate to display the experimental error as one standard deviation, and the data are shown in Fig. 1.

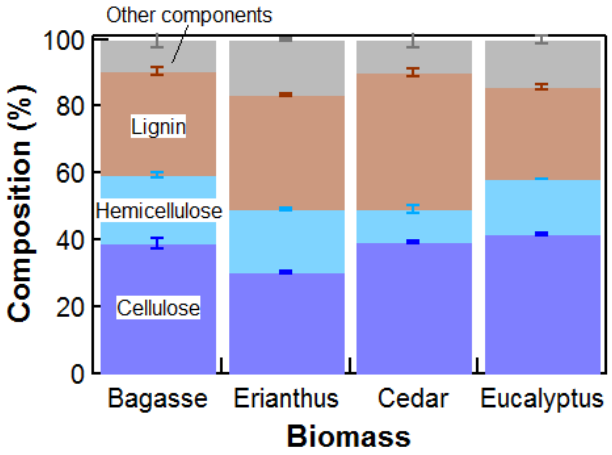

Fig. 1. Chemical composition of biomass samples

In the IL-pretreatment process, 0.1 g of lignocellulose and various amounts of [Emim][OAc] were mixed using a spatula for approximately 5 min at room temperature. The mixture was then heated at 130 °C for 3 h, as an optimized condition for bagasse (Aung *et al.* 2018). After the mixture was cooled down to room temperature, the IL was removed by washing with distilled water five times. Various lignocellulose-to-IL ratios of 1:1, 1:2, 1:3, 1:5, 1:10, and 1:20 (w/w) correspond to lignocellulosic concentrations of 50, 33, 25, 17, 9, and 5 wt%, respectively.

Methods

Structural assessments

The WAXS measurements were carried out using a NANO Viewer (IP system; Rigaku Corporation, Tokyo, Japan). The CuKα radiation source (λ = 0.154 nm) was employed at an applied voltage of 40 kV and a filament current of 30 mA. The lignocellulose samples were freeze-dried and then first packed into a Teflon cell (1-mm-thick) and sandwiched between two sheets of Kapton film. The samples irradiation times

were 1 h to 4 h. The crystallinity index (CrI) was obtained using the Segal method (Segal *et al.* 1959) as shown in Eq. 1,

$$\mathrm{CrI}_{\mathrm{WAXS}}\ (\%) = \frac{I_{\max} - I_{\mathrm{am}}}{I_{\max}} \times 100 \quad (1)$$

where I_{max} and I_{am} represent the X-ray intensities at the maximum (crystalline) and 2θ = 18.5° (amorphous), respectively. To evaluate peak position, a Gauss function was fitted to observed peaks.

The SSNMR measurements were carried out using a JNM-ECX 500II spectrometer (11.75 T; JEOL, Tokyo, Japan). The freeze-dried lignocellulose was placed in a 3.2-mm zirconia rotor (49 µL) to perform ^{13}C cross-polarization/magic-angle spinning (CP/MAS) measurements with an MAS speed of 10 kHz. These spectra were collected using a contact time of 2 ms and a recycle delay of 3 s. Each ^{13}C spectrum was the accumulation of 4096 to 16384 scans. The ^{13}C chemical shifts were determined by reference to adamantane (at δ 29.5 ppm for CH). The crystallinity index from the SSNMR measurements (CrI_{NMR}) was estimated based on the fraction of order (at δ 86.8 ppm to 92.4 ppm) to the total area of order and disorder (at δ 80.4 ppm to 86.8 ppm) for the C4 peak of cellulose. The fractions for the tg (trans-gauche), gt (gauche-trans), and gg (gauche-gauche) conformers of the C6 carbon site of cellulose were estimated in the regions of δ 64.2 ppm to 66.0 ppm, 61.7 ppm to 64.2 ppm, and 59.1 ppm to 61.7 ppm, respectively.

Acid hydrolysis

The procedure for acid hydrolysis of lignocellulose was followed from the authors' previous study (Endo *et al.* 2017). Approximately 3 mL of 0.5 M H_2SO_4 solution was placed in a sealed cell with 0.1 g lignocellulose and heated at 130 °C with a roller oven (RDV-TM2; SAN-AI Kagaku, Aichi, Japan). After heating for 4 h, the reaction was halted by placing the sample in an ice bath followed by centrifuging the hydrolysate for further analysis. The released glucose in the hydrolysate was detected by high pressure liquid chromatography (HPLC; Shimadzu Corporation, Kyoto, Japan) equipped with a refractive index detector and a CARBOSep CHO-682 column (Tokyo Chemical Industry Co., Tokyo, Japan). The analysis conditions in HPLC were as follows: the volume of the injected sample was 20 µL, the column was operated at 70 °C, and 0.0085 N H_2SO_4 solution was used in the mobile phase with a flow rate set at 0.4 mL/min. The hydrolysate measurements were taken in triplicate to display experimental error as one standard deviation.

Thermogravimetric analysis

Thermogravimetric analyses were performed with DTG-60AH (Shimadzu Corporation, Kyoto, Japan). Dried untreated biomass (4 to 5 mg) was placed in a platinum pan. The pan was heated to 1000 °C with the scan rate of 10 °C/min.

RESULTS AND DISCUSSION

WAXS Measurements

Figure 2(a) shows the WAXS patterns of untreated lignocellulose in addition to theoretical reference patterns of cellulose-I and cellulose-II (Nishiyama *et al.* 2002; French 2014). The cellulose-I and cellulose-II possess three intense peaks at 2θ values 14.9° ($1\bar{1}0$), 16.7° (110), 23.0° (200), and 12.2° ($1\bar{1}0$), 19.9° (110), and 22.1° (020), respectively. Native

cellulose takes the cellulose-I form, while it tends to transform to the more thermodynamically stable cellulose-II structure after IL pretreatments (Cheng *et al.* 2011; Samayam *et al.* 2011). All four biomass samples exhibited similar WAXS patterns that resemble cellulose-I. However, the peak for the (200) plane was shifted to a lower angle probably because of the presence of hemicellulose and lignin (Sun *et al.* 2014). It was noted that small sharp peaks sometimes appeared (*e.g.*, one at 27° for bagasse) that were assigned to some inorganic crystallized components contained in lignocellulose (Konsolakis *et al.* 2015).

The WAXS patterns of the lignocellulose in different loading amounts are displayed in Figs. 2(b through d). The behaviors with respect to loading amount in the grassy biomass (bagasse and erianthus) samples differed distinctively from the woody biomass (cedar and eucalyptus). The patterns for the grassy biomass gradually broadened with decreasing loading amount from 50 wt% to 5 wt%, and at the most dilute condition only one broad peak appeared centered at ca. 21°. In contrast, the WAXS patterns for the woody biomass abruptly changed between the 50 wt% and 33 wt% loading amounts. Even at the lower loading amounts, unlike the grassy biomass, a shoulder peak around 14° remained. This peak position was lower than the original (see Fig. 3(b)) sample, indicating the presence of the cellulose-II structure. Before proceeding with further discussion, it should be noted that the chemical composition of IL-pretreated biomass is not notably altered by changing the loading amount (Wu *et al.* 2011; da Silva *et al.* 2013; Ninomiya *et al.* 2013; Aung *et al.* 2018). Hence, the changes in WAXS pattern were attributed to the cellulose crystalline states.

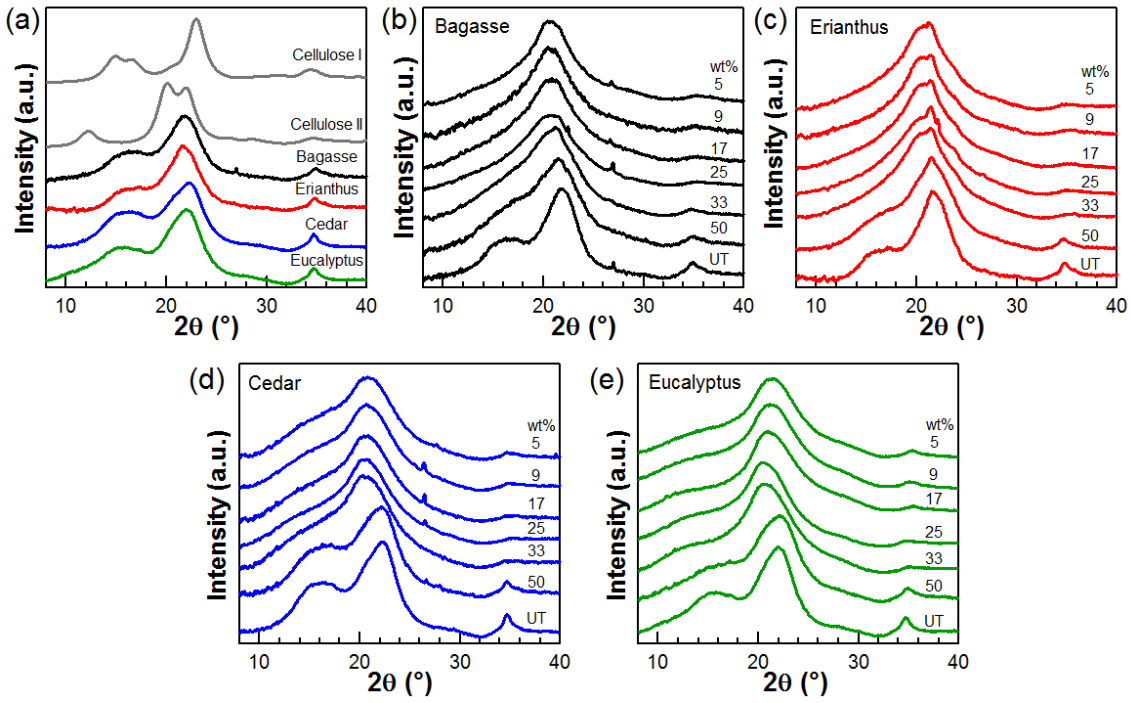

Fig. 2. (a) WAXS patterns of various untreated biomass and theoretical powder patterns of cellulose I and cellulose II (French 2014; Nishiyama *et al.* 2002). The colors used are consistent with the following figures, *i.e.*, black for bagasse, red for erianthus, blue for cedar, and green for eucalyptus; (b through e) WAXS patterns of untreated (UT) and pretreated biomass at various loading amounts.

To gain further insights for the peak change behaviors, peak analyses were performed. The peak position changes of the strong peak around 21° are shown in Fig. 3(a), and those of the shoulder peak for cedar and eucalyptus are shown in Fig. 3(b). These results highlighted the difference between the grassy and woody biomass samples. The intense peak was shifted gradually to low 2θ values from 50 wt% to 5 wt% loadings in the grassy biomass. These results were similar to those previously observed (Cheng *et al.* 2011), and were mainly attributable to the gradual change from cellulose-I to cellulose-II. The behavior for the woody biomass was more complex. After the abrupt change between 50 wt% and 33 wt% loadings, the peak position was shifted to a large angle with decreased biomass loadings. Because a large change was also observed for the shoulder peak from 50 wt% to 33 wt% (Fig. 3(b)), it indicated the transformation into the cellulose-II structure. This result strongly suggested that a large portion of cellulose-I was transformed to cellulose-II at the 33 wt% loading. At lower loadings, the peak position was gradually returned to higher angle (Fig. 3(a)), which was more prominent in eucalyptus than cedar. This behavior is rather unique, and a plausible explanation was the reformation of the cellulose-I structure at the lower loadings. Normally thermodynamically stable cellulose-II is formed first from cellulose-I *via* an amorphous state in IL pretreatments (Cheng *et al.* 2011; Samayam *et al.* 2011). However, there was a high energy barrier in this transformation due to the large difference in cellulose chain alignment; parallel for cellulose-I and antiparallel for cellulose-II. Then, occasionally the amorphous domains of cellulose dissolved in an IL return to cellulose-I after the IL is removed by washing (Lucas *et al.* 2011). It was noted that the large peak position shifting observed in eucalyptus may not have been explained only by the reformation of cellulose-I. The lattice expansion and shrinking of cellulose crystal can be involved in the peak shifting. The authors will discuss the crystal structural changes again in the SSNMR section, which support the abovementioned explanations.

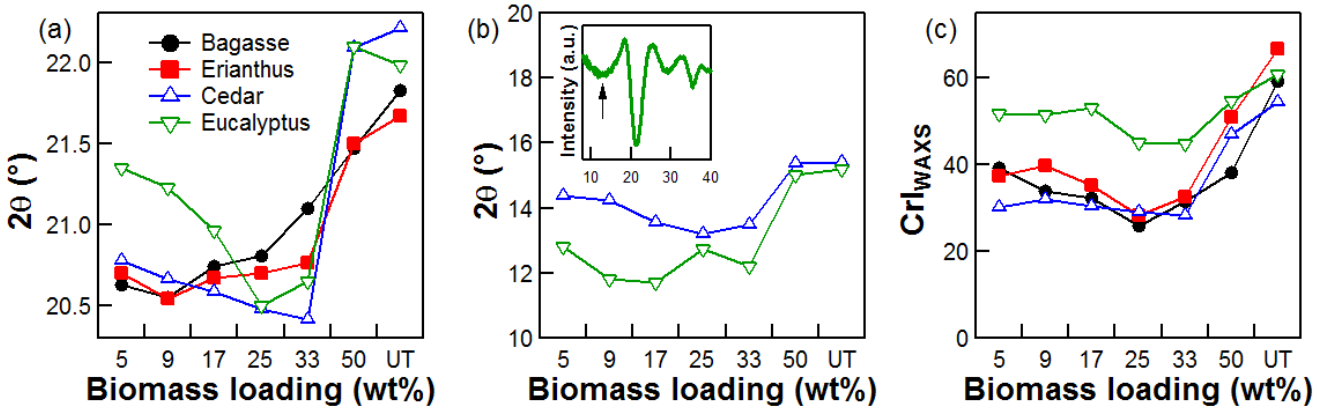

Fig. 3. Shifts of (a) the strong WAXS peak and (b) the weak shoulder peak. The inset shows the second derivative of the WAXS pattern of the 5 wt% eucalyptus sample after pattern smoothing operations (box smoothing), displayed as an example. The negative peak, indicated by an arrow, demonstrates the existence of the shoulder peak. (c) CrI estimated from the WAXS measurements with the Segal method.

The CrI of cellulose is considered to govern the cellulose accessibility, which is a factor of concern in this study. The CrI_{WAXS} values were estimated from the Segal method and are displayed in Fig. 3(c). As the authors previously reported, the CrI of pretreated bagasse was lower at the higher loadings of 17 to 33 wt% than the conventional 5 wt%

loading (Aung *et al.* 2018). The cellulose crystalline structure was mostly deconstructed even at the high loadings, which means that the majority of cellulose exists in the amorphous state even in the highly lignocellulose-loaded mixture (Endo *et al.* 2016). When the IL was removed from the mixture by washing, the recrystallization to cellulose-II was inhibited because of the restricted movements of the cellulose chain by a highly viscous environment (Aung *et al.* 2018; Endo *et al.* 2017). The CrI_{WAXS} values for erianthus as the grassy biomass also followed the same trend, *i.e.*, the lowest CrI_{WAXS} appeared at 25 wt% biomass loading. This also may be the case for the woody biomass, but it was ambiguous for cedar. The result for eucalyptus needed more caution as the Segal method was employed which simply uses two peak intensities to estimate the CrI_{WAXS}. The peak position shifts affect the CrI_{WAXS} values, particularly for eucalyptus. Lowering the strongest peak made I_{max} large which caused an underestimation of the CrI_{WAXS} values.

SSNMR Measurements

To ensure the changes in the CrI behaviors, ^{13}C SSNMR experiments were performed. From the NMR spectra, the crystallinity of cellulose was estimated at the molecular level. These values would be less sensitive to the crystalline states (*e.g.*, allomorphs and lattice size changes) as well as the presence of hemicellulose and lignin.

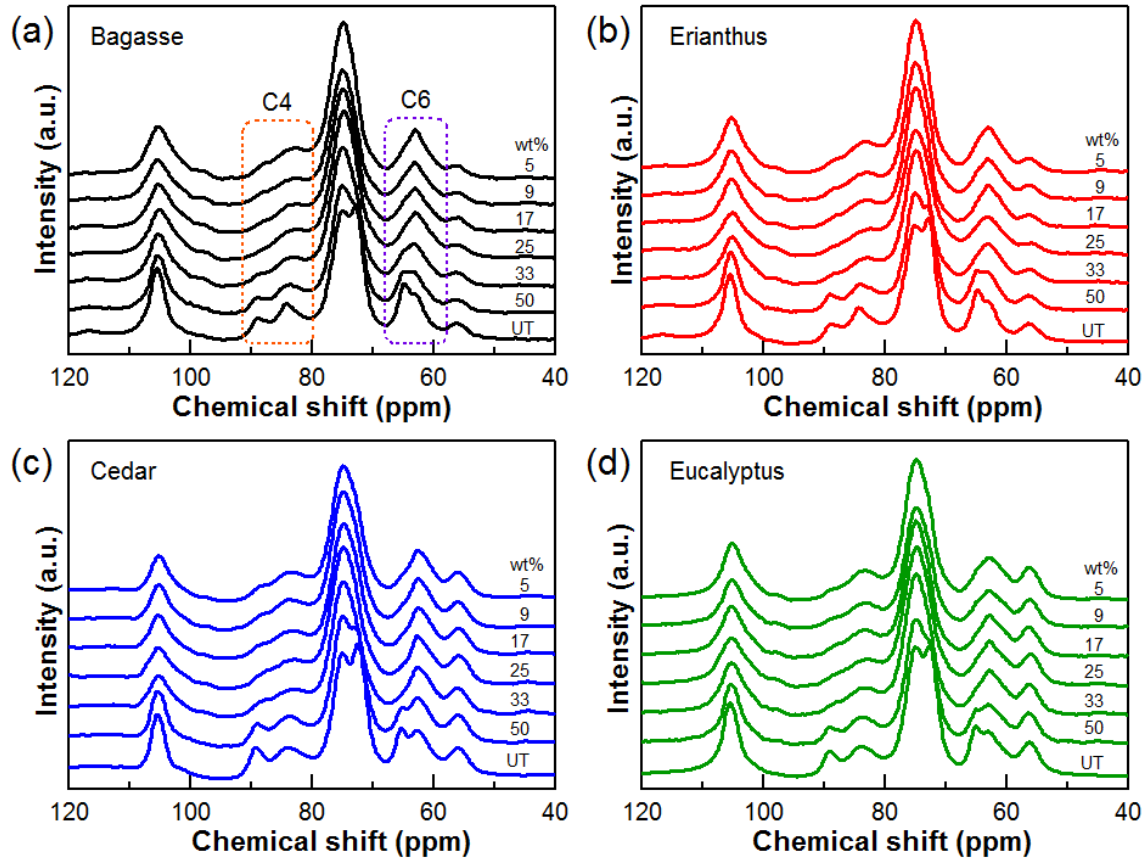

Fig. 4. ^{13}C CP/MAS spectra of untreated (UT) and pretreated (a) bagasse, (b) erianthus, (c) cedar, and (d) eucalyptus at different loading amounts

Figure 4 shows the ^{13}C cross-polarization magic angle spinning (CP/MAS) spectra of the untreated and pretreated lignocellulose sample. The strong peaks found at δ 60 to 110 ppm were mainly from cellulose. The C-4 carbon in the glucose unit splits into two regions, as assigned to ordered and disordered (*i.e.*, in amorphous or surface domains) conformations (Horii *et al.* 1982; Larsson *et al.* 1997). The ordered component relative to the total of the ordered and disordered components was used as the CrI estimated from NMR (CrI_{NMR}). The C-6 site also splits into three, which in turn provides useful information at the molecular level. The different hydroxymethyl group conformations of cellulose (tg, gt, and gg) divide the C-6 carbon peak into three regions (Horii *et al.* 1983; Fernandes *et al.* 2011). The tg conformer is mainly present in the crystalline core of cellulose-I (Nishiyama *et al.* 2002, 2003; Wang *et al.* 2016), whereas cellulose-II has the gt conformation in its core (Langan *et al.* 2001). The gt and gg conformers are both present on the crystal surfaces (Horii *et al.* 1983; Viëtor *et al.* 2002; Newman and Davidson 2004), but the gg conformer exists predominantly in the amorphous domain (Mazeau and Heux 2003; Newman and Davidson 2004; Idström *et al.* 2016).

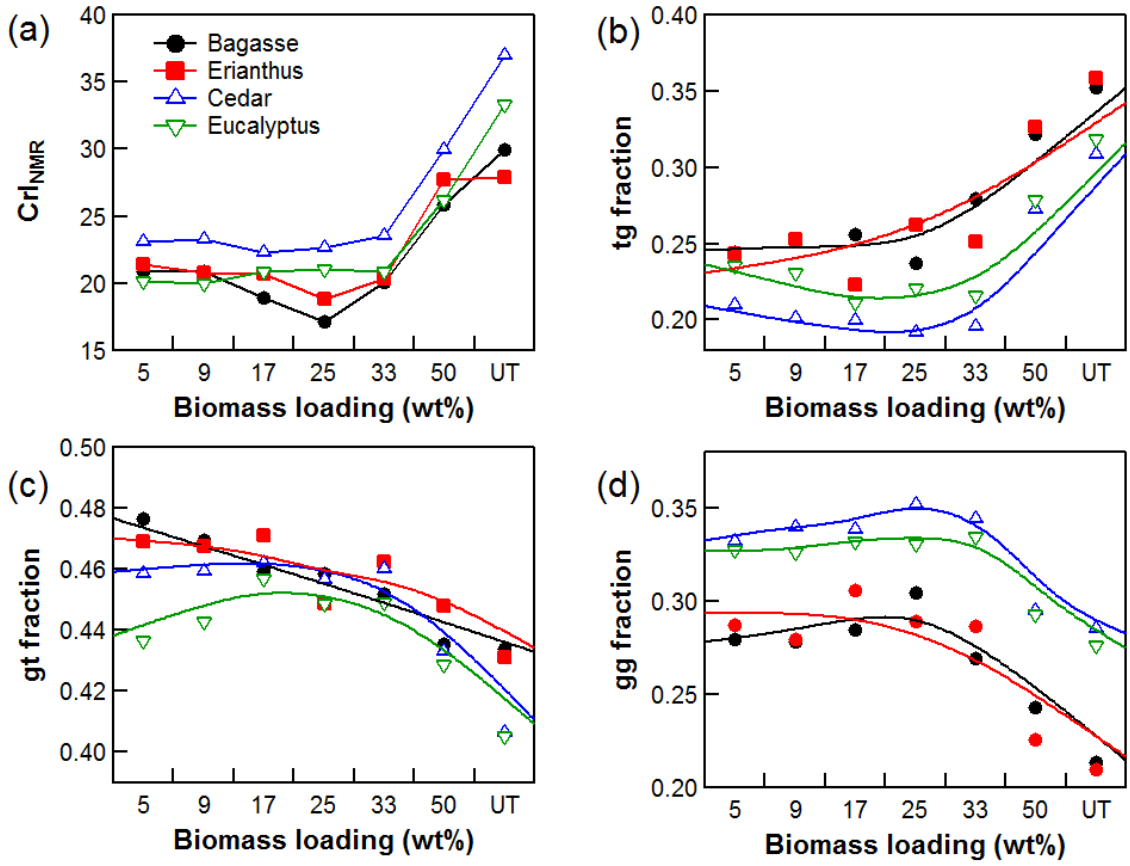

Fig. 5. (a) CrI_{NMR} values based on the C-4 peak area, and the fractions of the (b) tg, (c) gt, and (d) gg conformers of the hydroxymethyl group of cellulose estimated based on the C-6 peak area against loading amount. The data for (b through d) are interpolated by smoothing spline displayed as solid lines.

Figure 5 summarizes the peak analysis results from the SSNMR spectra. The CrI_{NMR} values (Fig. 5(a)) were mostly consistent with those from WAXS except for eucalyptus. The CrI_{NMR} of eucalyptus was independent of biomass loading amounts

between 33 wt% and 5 wt%. Because the Segal method in the WAXS measurement is affected by peak shift changes and the SSNMR method is less sensitive to undesired effects, it was concluded that the CrI values of the pretreated eucalyptus did not change in the range of 33 wt% to 5 wt%. In contrast, the pretreated cedar showed minimum CrI, *e.g.*, 17 wt%, however, the behavior was closer to that of eucalyptus rather than that of the grassy biomass.

The fraction changes of the hydroxymethyl group conformations, tg, gt, and gg, are displayed in Figs. 5(b–d). There were three components that existed in the relatively narrow chemical shift range, besides, a shoulder of the large peak at *ca.* 75 ppm that mainly came from C-2, C-3, and C-5 of cellulose also existed in the same range. This is probably the reason for that the data, particularly for erianthus (red in the figures), were rather scattered. Therefore, the data were interpolated by a smoothing spline, and displayed as solid lines in the figures. For the same reason, much attention was not given to the absolute values. The results from the different biomass samples for the tg (mainly exists in cellulose-I) and gt (mainly exists in cellulose-II) conformations can be roughly classified into two categories as the grassy and woody biomass, as was seen in the WAXS results. For the grassy biomass, relatively monotonic changes of the tg and gt fractions were observed. This indicated the gradual transformation from cellulose-I to cellulose-II against the loading, consistent with the WAXS results. The plots for the woody biomass showed a basin and a bell-shape for of the tg and gt fractions, respectively. This corresponded to that the original cellulose-I transformed into cellulose-II from untreated to 25 wt%. Below this concentration, the reformation of cellulose-I occurred as discussed in the WAXS measurements section.

The gg fraction changes (Fig. 5(d)) provided a similar plot for all biomass samples studied and this would not be discussed in the two classification (grass and wood) framework. As discussed in the previous paper (Aung *et al.* 2018), the bagasse sample (black in the figures) had a maximum at the high loading of 25 wt%. The gg conformer mainly existed in the amorphous domain and crystal surfaces. The two important cellulose accessibility parameters, CrI and specific surface area, also showed a minimum or maximum value around the high loading. Consequently a maximum value for the gg fraction was observed (Endo *et al.* 2017). When taking a look at other biomass that were investigated here, such a maximum was also observed for erianthus and cedar, but was ambiguous for eucalyptus.

Acid Hydrolysis and its Relation with Cellulose Structural State

Figure 6(a) shows the glucose yields of the untreated and pretreated biomass samples hydrolyzed by sulfuric acid as the catalyst during 4 h. The glucose yields for bagasse at the same hydrolysis condition became maximum during 8 h to 16 h, depending on the loading amount (Aung *et al.* 2018). Because a general trend of biomass reactivity for hydrolysis follows grass > hardwood > softwood (Zhu and Pan 2010), the glucose yields at 4 h can be approximated to the initial reaction rate of the hydrolysis. The glucose yields were plotted against the CrI estimated from WAXS and SSNMR as well as the gg fraction as shown in Figs. 6(b through d). Good correlations were mostly obtained except for that between the glucose and CrI_{WAXS} for eucalyptus ($R^2 = 0.50$), due to the large WAXS peak shift as discussed before.

The pretreated bagasse showed a higher glucose yield at higher loadings of 17 wt% to 33 wt% than the conventional 5 wt% loading (black in Fig. 6) because of the resultant lower cellulose crystallinity (Aung *et al.* 2018). The glucose yields for eucalyptus were mostly the same in the range of 5 wt% to 25 wt%. This was reasonable because the CrI as

well as the gg fraction did not change much in this region (Figs. 5(a) and 5(d)). With the pretreatments at 5 wt% and 9 wt% loadings, the eucalyptus produced more glucose than the bagasse, which was contradictory to the general trend of grassy and woody biomass reactivity (Zhu and Pan 2010). This implies that, unlike bagasse, the recrystallization of cellulose-II was suppressed and cellulose in the pretreated eucalyptus remained amorphous even at the lower loadings. Characteristics of hemicellulose and lignin matrices in the eucalyptus could be responsible for this.

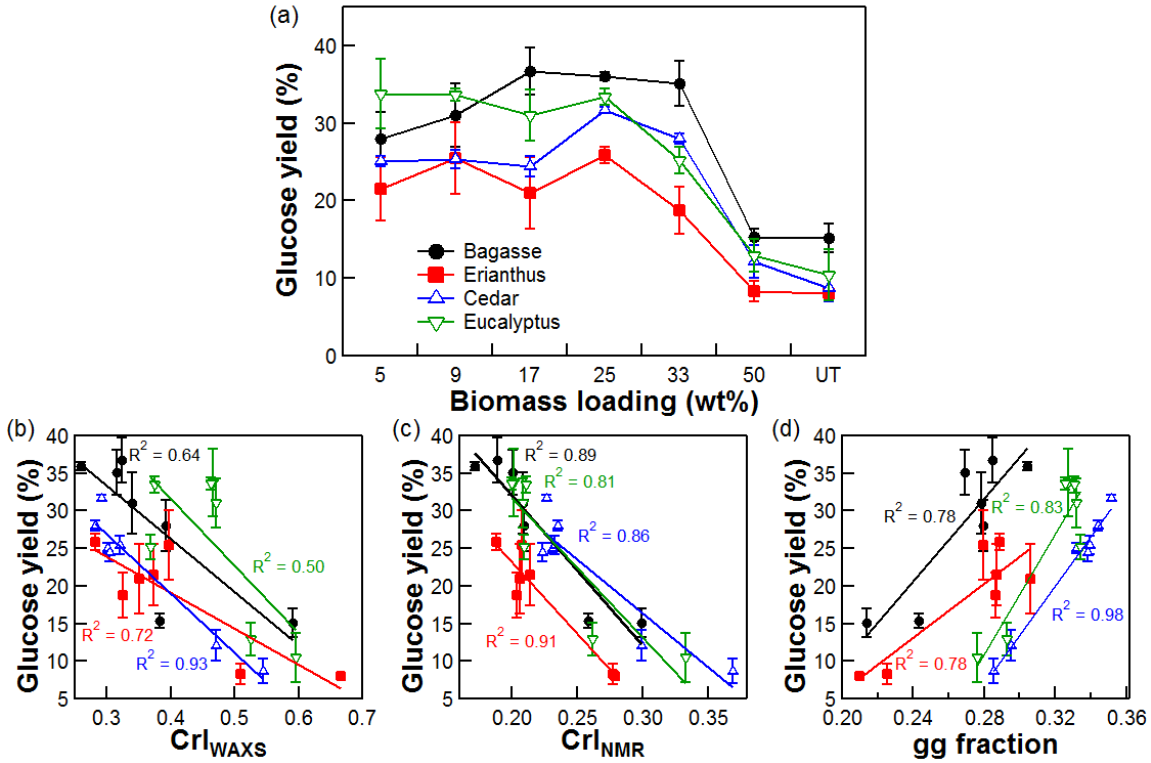

Fig. 6. (a) Glucose yields of untreated (UT) and pretreated biomass at the reaction time of 4 h. The values were set at 100% when cellulose in untreated lignocellulose was completely transformed into glucose. (b) CrI_{WAXS}, (c) CrI_{NMR}, and (d) the gg fraction changes against the glucose yield.

Even though cedar is a woody biomass and the structural changes against the biomass loading amount that occurred were similar to eucalyptus, the glucose yield curve for cedar resembled that for bagasse, *i.e.*, the glucose yield was the highest at the high loading of 25 wt%. Precisely, the slightly lower CrI and higher gg fraction at higher loadings than 5 wt% were observed for cedar (Figs. 3(c), 5(a), and 5(d)). However, it should be pointed out that these slight differences might not be the main reason. Although cellulose crystallinity is truly an important factor for the recalcitrance, other cellulose accessibility parameters, such as specific surface area and structures of hemicellulose and lignin (Mosier *et al.* 2005; Kumar *et al.* 2009), must also be considered.

The results from erianthus were counterintuitive. The samples of erianthus and bagasse were categorized as grassy biomass, and the former showed very similar structural behaviors of cellulose to the latter when the loading amount was increased. However, the glucose yields of the pretreated erianthus were the lowest among all the biomass samples

tested, and whether the glucose yield was higher at higher loadings than the 5 wt% loading was rather unclear. An explanation can be made in terms of the neutralizing ability; each biomass had different abilities to neutralize the acid used. The neutralizing ability is correlated with ash content (Esteghlalian *et al.* 1997), and erianthus was reported to possess a high ash content (Yamamura *et al.* 2013). The authors conducted thermogravimetric analyses on bagasse and erianthus, and confirmed the higher ash content of erianthus (9.3%) than that of bagasse (5.9%) when heated to 1000 °C, the result of which was also in line with the fraction of the other components in the compositional analyses (Fig. 1).

CONCLUSIONS

The IL pretreatments of four lignocellulosic biomass samples, bagasse, erianthus, cedar, and eucalyptus were conducted at various biomass loadings. The structural investigations were performed with WAXS and SSNMR analyses:

1. The results indicated that the cellulose structural changes in the pretreated biomass responded differently between the grassy (bagasse and erianthus) and the woody (cedar and eucalyptus) biomass against the loading amount.
2. The gradual transformation from cellulose-I to cellulose-II occurred in the pretreated bagasse and erianthus, corresponding to the gradual change in loading amount. They showed the minimum CrI value at the 25 wt% loading that was notably higher than the conventional loading of 5 wt%.
3. Unlike at 50 wt%, a large portion of cellulose-I was transformed into cellulose-II at 33 wt% for the pretreated cedar and eucalyptus. Below 33 wt%, the reformation of cellulose-I was observed. The CrI values did not show a clear minimum at the high loadings, whereas there might be a slight basin for the pretreated cedar.
4. Hydrolysis efficiency catalyzed by acid for the pretreated biomass was also evaluated. Except for erianthus, the results on the glucose yields reflected the same changes in the CrI and other structural parameters of cellulose, *i.e.*, bagasse and cedar showed higher glucose yields at higher loading amounts to some extents while eucalyptus provided a constant value in the range of 5 wt% to 25 wt%. The counterintuitive behavior for erianthus was attributed to the high neutralizing ability of the sample.

ACKNOWLEDGMENTS

This study was financially supported in part by the Advanced Low Carbon Technology Research and Development Program (ALCA) (Grant No. 2100040), the Cross-ministerial Strategic Innovation Promotion Program (SIP), and the Center of Innovation Program "Construction of next-generation infrastructure using innovative materials: Realization of safe and secure society that can coexist with the Earth for centuries," from the Japan Science and Technology Agency, and also by the Asahi Glass Foundation. The authors thank Dr. Nagasawa from the National Agriculture and Food Research Organization for the kind supply of erianthus.

REFERENCES CITED

Aung, E. M., Endo, T., Fujii, S., Kuroda, K., Ninomiya, K., and Takahashi, K. (2018). "Efficient pretreatment of bagasse at high loading in an ionic liquid," *Ind. Crops Prod.* 119, 243-248. DOI: 10.1016/j.indcrop.2018.04.006

Baral, N. R., and Shah, A. (2016). "Techno-economic analysis of cellulose dissolving ionic liquid pretreatment of lignocellulosic biomass for fermentable sugars production," *Biofuels, Bioprod. Biorefin.* 10(1), 70-88. DOI: 10.1002/bbb.1622

Brandt, A., Grasvik, J., Hallett, J. P., and Welton, T. (2013). "Deconstruction of lignocellulosic biomass with ionic liquids," *Green Chem.* 15(3), 550-583. DOI: 10.1039/C2GC36364J

Cheng, G., Varanasi, P., Li, C., Liu, H., Melnichenko, Y. B., Simmons, B. A., Kent, M. S., and Singh, S. (2011). "Transition of cellulose crystalline structure and surface morphology of biomass as a function of ionic liquid pretreatment and its relation to enzymatic hydrolysis," *Biomacromolecules* 12(4), 933-941. DOI: 10.1021/bm101240z

Cruz, A. G., Scullin, C., Mu, C., Cheng, G., Stavila, V., Varanasi, P., Xu, D., Mentel, J., Chuang, Y.-D., Simmons, B. A., *et al.* (2013). "Impact of high biomass loading on ionic liquid pretreatment," *Biotechnol. Biofuels* 6(1), 52. DOI: 10.1186/1754-6834-6-52

da Silva, A. S. A., Teixeira, R. S. S., Endo, T., Bon, E. P. S., and Lee, S.-H. (2013). "Continuous pretreatment of sugarcane bagasse at high loading in an ionic liquid using a twin-screw extruder," *Green Chem.* 15(7), 1991-2001. DOI: 10.1039/C3GC40352A

Endo, T., Aung, E. M., Fujii, S., Hosomi, S., Kimizu, M., Ninomiya, K., and Takahashi, K. (2017). "Investigation of accessibility and reactivity of cellulose pretreated by ionic liquid at high loading," *Carbohydr. Polym.* 176, 365-373. DOI: 10.1016/j.carbpol.2017.08.105

Endo, T., Hosomi, S., Fujii, S., Ninomiya, K., and Takahashi, K. (2016). "Anion bridging-induced structural transformation of cellulose dissolved in ionic liquid," *J. Phys. Chem. Lett.* 7(24), 5156-5161. DOI: 10.1021/acs.jpclett.6b2504

Esteghlalian, A., Hashimoto, A. G., Fenske, J. J., and Penner, M. H. (1997). "Modeling and optimization of the dilute-sulfuric-acid pretreatment of corn stover, poplar and switchgrass," *Bioresour. Technol.* 59(2), 129-136. DOI: 10.1016/S0960-8524(97)81606-9

Fernandes, A. N., Thomas, L. H., Altaner, C. M., Callow, P., Forsyth, V. T., Apperley, D. C., Kennedy, C. J., and Jarvis, M. C. (2011). "Nanostructure of cellulose microfibrils in spruce wood," *Proc. Natl. Acad. Sci. U.S.A.* 108(47), E1195-E1203. DOI: 10.1073/pnas.1108942108

French, A. D. (2014). "Idealized powder diffraction patterns for cellulose polymorphs," *Cellulose* 21(2), 885-896. DOI: 10.1007/s10570-013-0030-4

Haykir, N. I., and Bakir, U. (2013). "Ionic liquid pretreatment allows utilization of high substrate loadings in enzymatic hydrolysis of biomass to produce ethanol from cotton stalks," *Ind. Crops Prod.* 51, 408-414. DOI: 10.1016/j.indcrop.2013.10.017

Horii, F., Hirai, A., and Kitamaru, R. (1982). "Solid-state high-resolution 13C-NMR studies of regenerated cellulose samples with different crystallinities," *Polym. Bull.* 8(2-4), 163-170. DOI: 10.1007/BF00263023

Horii, F., Hirai, A., and Kitamaru, R. (1983). "Solid-state 13C-NMR study of conformations of oligosaccharides and cellulose - Conformation of CH_2OH group about the exo-cyclic C-C bond," *Polym. Bull.* 10(7-8), 357-361. DOI: 10.1007/BF00281948

Idström, A., Schantz, S., Sundberg, J., Chmelka, B. F., Gatenholm, P., and Nordstierna, L. (2016). "13C NMR assignments of regenerated cellulose from solid-state 2D NMR spectroscopy," *Carbohydr. Polym.* 151, 480-487. DOI:10.1016/j.carbpol.2016.05.107

Kilpeläinen, I., Xie, H., King, A., Granstrom, M., Heikkinen, S., and Argyropoulos, D. S. (2007). "Dissolution of wood in ionic liquids," *J. Agric. Food. Chem.* 55(22), 9142-9148. DOI: 10.1021/jf071692e

Konsolakis, M., Kaklidis, N., Marnellos, G. E., Zaharaki, D., and Komnitsas, K. (2015). "Assessment of biochar as feedstock in a direct carbon solid oxide fuel cell," *RSC Adv.* 5(90), 73399-73409. DOI: 10.1039/c5ra13409a

Kumar, P., Barrett, D. M., Delwiche, M. J., and Stroeve, P. (2009). "Methods for pretreatment of lignocellulosic biomass for efficient hydrolysis and biofuel production," *Ind. Eng. Chem. Res.* 48(8), 3713-3729. DOI: 10.1021/ie801542g

Langan, P., Nishiyama, Y., and Chanzy, H. (2001). "X-ray structure of mercerized cellulose II at 1 Å resolution," *Biomacromolecules* 2(2), 410-416. DOI: 10.1021/bm005612q

Larsson, P. T., Wickholm, K., and Iversen, T. (1997). "A CP/MAS13C NMR investigation of molecular ordering in celluloses," *Carbohydr. Res.* 302(1–2), 19-25. DOI: 10.1016/S0008-6215(97)00130-4

Li, C., Tanjore, D., He, W., Wong, J., Gardner, J. L., Sale, K. L., Simmons, B. A., and Singh, S. (2013). "Scale-up and evaluation of high solid ionic liquid pretreatment and enzymatic hydrolysis of switchgrass," *Biotechnol. Biofuels* 6(1), 154. DOI: 10.1186/1754-6834-6-154

Lucas, M., Wagner, G. L., Nishiyama, Y., Hanson, L., Samayam, I. P., Schall, C. A., Langan, P., and Rector, K. D. (2011). "Reversible swelling of the cell wall of poplar biomass by ionic liquid at room temperature," *Bioresour. Technol.* 102(6), 4518-4523. DOI: 10.1016/j.biortech.2010.12.087

Mazeau, K., and Heux, L. (2003). "Molecular dynamics simulations of bulk native crystalline and amorphous structures of cellulose," *J. Phys. Chem. B* 107(10), 2394-2403. DOI: 10.1021/jp0219395

Mosier, N., Wyman, C., Dale, B., Elander, R., Lee, Y. Y., Holtzapple, M., and Ladisch, M. (2005). "Features of promising technologies for pretreatment of lignocellulosic biomass," *Bioresour. Technol.* 96(6), 673-686. DOI: 10.1016/j.biortech.2004.06.025

Newman, R. H., and Davidson, T. C. (2004). "Molecular conformations at the cellulose-water interface," *Cellulose* 11(1), 23-32. DOI: 10.1023/B:CELL.0000014778.49291.c6

Ninomiya, K., Soda, H., Ogino, C., Takahashi, K., and Shimizu, N. (2013). "Effect of ionic liquid weight ratio on pretreatment of bamboo powder prior to enzymatic saccharification," *Bioresour. Technol.* 128, 188-92. DOI: 10.1016/j.biortech.2012.10.097

Nishiyama, Y., Langan, P., and Chanzy, H. (2002). "Crystal structure and hydrogen-bonding system in cellulose Iβ from synchrotron X-ray and neutron fiber diffraction," *J. Am. Chem. Soc.* 124(31), 9074-9082. DOI: 10.1021/ja0257319

Nishiyama, Y., Sugiyama, J., Chanzy, H., and Langan, P. (2003). "Crystal structure and hydrogen bonding system in cellulose iα from synchrotron X-ray and neutron fiber diffraction," *J. Am. Chem. Soc.* 125(47), 14300-14306. DOI: 10.1021/ja037055w

Qiu, Z., Aita, G. M., and Mahalaxmi, S. (2014). "Optimization by response surface methodology of processing conditions for the ionic liquid pretreatment of energy cane bagasse," *J. Chem. Technol. Biotechnol.* 89(5), 682-689. DOI: 10.1002/jctb.4167

Reddy, P. (2015). "A critical review of ionic liquids for the pretreatment of lignocellulosic biomass," *S. Afr. J. Sci.* 111(11-12), 20150083. DOI: 10.17159/sajs.2015/20150083

Ren, H., Zong, M.-H., Wu, H., and Li, N. (2016). "Efficient pretreatment of wheat straw using novel renewable cholinium ionic liquids to improve enzymatic saccharification," *Ind. Eng. Chem. Res.* 55(6), 1788-1795. DOI: 10.1021/acs.iecr.5b03729

Samayam, I. P., Hanson, B. L., Langan, P., and Schall, C. A. (2011). "Ionic-liquid induced changes in cellulose structure associated with enhanced biomass hydrolysis," *Biomacromolecules* 12(8), 3091-3098. DOI: 10.1021/bm200736a

Segal, L., Creely, J. J., Martin, A. E., Jr., and Conrad, C. M. (1959). "An empirical method for estimating the degree of crystallinity of native cellulose using the x-ray diffractometer," *Text. Res. J.* 29, 786-94. DOI: 10.1177/004051755902901003

Sluiter, A., Hames, B., Ruiz, R., Scarlata, C., Sluiter, J., Templeton, D., and Crocker, D. (2012). "Determination of structural carbohydrates and lignin in biomass," National Renewable Energy Laboratory.

Sun, N., Parthasarathi, R., Socha, A. M., Shi, J., Zhang, S., Stavila, V., Sale, K. L., Simmons, B. a., and Singh, S. (2014). "Understanding pretreatment efficacy of four cholinium and imidazolium ionic liquids by chemistry and computation," *Green Chem.* 16(5), 2546-2546. DOI: 10.1039/c3gc42401d

Swatloski, R. P., Spear, S. K., Holbrey, J. D., and Rogers, R. D. (2002). "Dissolution of cellulose with ionic liquids," *J. Am. Chem. Soc.* 124, 4974-4975. DOI: 10.1021/ja025790m

Uju, Abe, K., Uemura, N., Oshima, T., Goto, M., and Kamiya, N. (2013). "Peracetic acid-ionic liquid pretreatment to enhance enzymatic saccharification of lignocellulosic biomass," *Bioresour. Technol.* 138, 87-94. DOI: 10.1016/j.biortech.2013.03.147

Viëtor, R. J., Newman, R. H., Ha, M. A., Apperley, D. C., and Jarvis, M. C. (2002). "Conformational features of crystal-surface cellulose from higher plants," *Plant J.* 30(6), 721-731. DOI: 10.1046/j.1365-313X.2002.01327.x

Wang, H., Gurau, G., and Rogers, R. D. (2012). "Ionic liquid processing of cellulose," *Chem. Soc. Rev.* 41(4), 1519-1537. DOI: 10.1039/c2cs15311d

Wang, S., You, T., Xu, F., Chen, J., and Yang, G. (2015). "Optimization of [Amim]Cl pretreatment conditions for maximum glucose recovery from hybrid pennisetum by response surface methodology," *BioResources* 10(4), 7021-7037. DOI: 10.15376/biores.10.4.7021-7037

Wang, T., Yang, H., Kubicki, J. D., and Hong, M. (2016). "Cellulose structural polymorphism in plant primary cell walls investigated by high-field 2D solid-state NMR spectroscopy and density functional theory calculations," *Biomacromolecules* 17(6), 2210-2222. DOI: 10.1021/acs.biomac.6b00441

Wu, H., Mora-Pale, M., Miao, J., Doherty, T. V., Linhardt, R. J., and Dordick, J. S. (2011). "Facile pretreatment of lignocellulosic biomass at high loadings in room

temperature ionic liquids," *Biotechnol. Bioeng.* 108(12), 2865-2875. DOI: 10.1002/bit.23266

Yamamura, M., Noda, S., Hattori, T., Shino, A., Kikuchi, J., Takabe, K., Tagane, S., Gau, M., Uwatoko, N., Mii, M., *et al.* (2013). "Characterization of lignocellulose of *Erianthus arundinaceus* in relation to enzymatic saccharification efficiency," *Plant Biotechnol.* 30(1), 25-35. DOI: 10.5511/plantbiotechnology.12.1127a

Zhang, J., Wang, Y., Zhang, L., Zhang, R., Liu, G., and Cheng, G. (2014). "Understanding changes in cellulose crystalline structure of lignocellulosic biomass during ionic liquid pretreatment by XRD," *Bioresour. Technol.* 151, 402-405. DOI: 10.1016/j.biortech.2013.10.009

Zhu, J. Y., and Pan, X. J. (2010). "Woody biomass pretreatment for cellulosic ethanol production: Technology and energy consumption evaluation," *Bioresour. Technol.* 101(13), 4992-5002. DOI: 10.1016/j.biortech.2009.11.007

Article submitted: May 30, 2018; Peer review completed: July 7, 2018; Revised version received and accepted: July 12, 2018; Published: July 17, 2018.
DOI: 10.15376/biores.13.3.6663-6677